

Nanoscale Spontaneous Patterning

Z. C. Feng¹ and Y. Charles Li²

Received 9 November 2005; accepted 6 March 2006
Published Online: May 3, 2006

The SMB equation describing nanoscale spontaneous patterning is studied both analytically and numerically. In contradiction to the claim in the original SMB paper [D. Srolovitz, A. Mazor, B. Bukiet, *J. Vac. Sci. Technol. A*6(4) (1988), 2371–2380.] that some steady states are stable, we found that all the steady states are unstable. A dynamical system reason for this is given. We also found that typical small initial data solutions undergo an exponential growth followed by an almost linear growth. Such a feature is consistent with the experimental data in the paper [J. Erlebacher et al., *J. Vac. Sci. Technol.*, A18(1) (2000), 115–120, Figure 3]. On the other hand, we never observed the decay portion of the numerical solution reported in this paper. We invent an elegant energy principle which supports our findings.

KEY WORDS: Nanoscale rippling, SMB equation, energy principle

1. INTRODUCTION

Spontaneous formation of nanoscale patterns on ion-bombarded surfaces has great potentials in nano-technology.⁽³⁾ The mechanism of such pattern formations is a balance between surface roughening induced by the ion beam, and surface relaxation due to the viscosity of the ion. A measure of the surface roughening is the curvature of the surface, while a measure of the surface relaxation is the second derivative of the curvature with respect to surface arc length. By considering rippled patterns, i.e. one-dimensional patterns, the SMB (Srolovitz-Mazor-Bukiet) equation was derived in.⁽⁴⁾ Although relevant, the SMB equation is far more complicated than the Cahn–Hilliard equation⁽²⁾ or the Allen–Cahn equation.⁽¹⁾ The SMB equation is a parabolic equation with a semi-definite coefficient. This

¹Department of Mechanical and Aerospace Engineering, University of Missouri, Columbia, MO 65211; e-mail: fengf@missouri.edu

²Department of Mathematics, University of Missouri, Columbia, MO 65211; e-mail: cli@math.missouri.edu

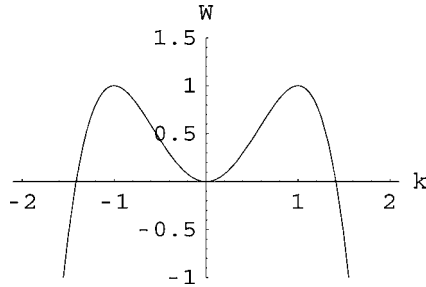


Fig. 1. The graph of the dispersion relation.

semi-definite nature supports ever growing solutions. In fact, typical solutions of SMB equation are ever growing. We invent an elegant energy principle which clearly shows that the semi-definite coefficient can support ever growing solutions. This ever growing nature is in agreement with experiments [Figure 3 of ⁽³⁾]. Typically the amplitude of the most unstable mode undergoes an exponential growth followed by a linear growth. Our growth curve will fit the experimental curve perfectly if scaled by a factor of 10^{-3} [Figure 3 of ⁽³⁾]. The transition from exponential growth to linear growth happens around $t = 10$. We do not know if the experimental curve in [Figure 3 of ⁽³⁾] has a factor of 10^{-3} error. On the other hand, we never observed the decay portion on the numerical growth curve in [Figure 3 of ⁽³⁾]. We also studied the steady states of the SMB equation. In contradiction to the claim in the original SMB paper⁽⁴⁾ that some non-zero steady states are stable, we found that all non-zero steady states are unstable. A clear dynamical system reason for the instability will be given too. Thus the non-zero steady states are not the final states of the ripples. No matter what initial condition to start with, the most unstable mode soon dominates. As time goes on, the solutions develop kinks on their spatial profiles.

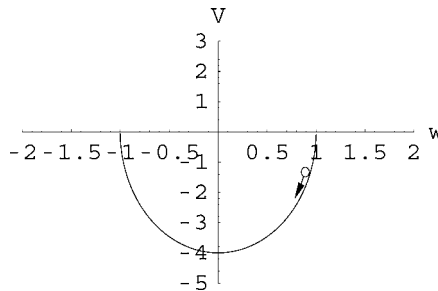


Fig. 2. The intuition of a ball sliding along a well.

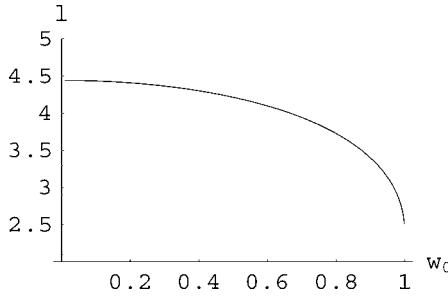


Fig. 3. The spatial period of the steady states as a function of w_0 .

2. ANALYSIS

The Srolovitz-Mazor-Bukiet (SMB) equation can be written in the following form

$$h_t = -\partial_x[f(h_x)(2h_x + \partial_x^2[h_x f(h_x)]), \tag{1}$$

where $f(z) = (1 + z^2)^{-1/2}$ and h is the scaled height profile in the moving frame of the average ripple position. Introduce $u = h_x$, one gets

$$u_t = -\partial_x^2[f(u)(2u + \partial_x^2[uf(u)]), \tag{2}$$

where again $f(u) = (1 + u^2)^{-1/2}$. For both Eqs. (2.1) and (2.2), periodic boundary condition can be imposed,

$$h(t, x + L) = h(t, x), \quad u(t, x + L) = u(t, x),$$

where L is some spatial period. In fact, both h and u have zero spatial mean,

$$\int_0^L h \, dx = \int_0^L u \, dx = 0.$$

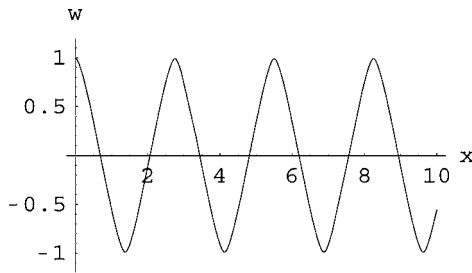


Fig. 4. The steady state profile for $w_0 = 0.99$.

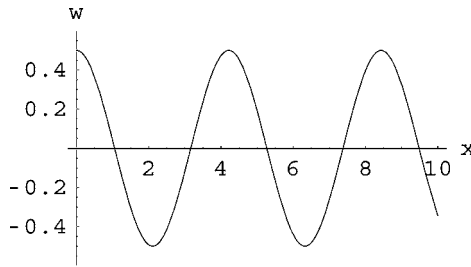


Fig. 5. The steady state profile for $w_0 = 0.5$.

Eq. (2.2) can be rewritten in the form

$$u_t = -(1 + u^2)^{-2}u_{xxxx} + G$$

where

$$G = 14(1 + u^2)^{-3}uu_xu_{xxx} + 10(1 + u^2)^{-3}uu_{xx}^2 + (19 - 95u^2)(1 + u^2)^{-4}u_x^2u_{xx} - (54 - 90u^2)(1 + u^2)^{-5}uu_x^4 - 2(1 + u^2)^{-3/2}u_{xx} + 6(1 + u^2)^{-5/2}uu_x^2.$$

Thus SMB is a parabolic equation with a semi-definite coefficient $(1 + u^2)^{-2}$. When $|u| \rightarrow \infty$, this coefficient approaches zero. This semi-definite nature can support ever growing solutions. In fact, our later numerics shows that typical solutions are indeed ever growing. The energy principle presented in the next section clearly shows the mechanism for ever growing. The following are some interesting identities related to the function $f(u) = (1 + u^2)^{-1/2}$,

$$u[uf]_x = -f_x, \quad [uf]_x = u_x f^3, \quad uu_x + f_x f^{-3} = 0.$$

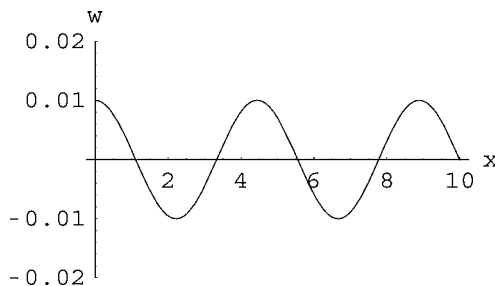


Fig. 6. The steady state profile for $w_0 = 0.01$.

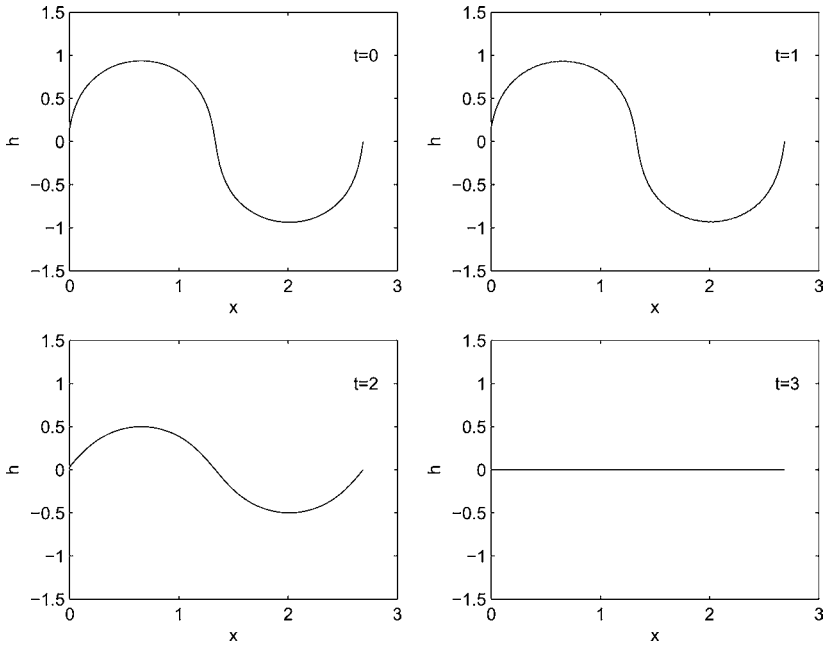


Fig. 7. The initial profile is the steady state profile for $u_0 = 8.0$ corresponding to $w_0 = 0.99227788$ via the transform $w_0 = \frac{u_0}{\sqrt{1+u_0^2}}$. No explicit initial perturbation is added. But the numerical error will introduce perturbations. The profile does not change much from $t = 0$ to $t = 1$. At $t = 3$, profile essentially approaches zero. The initial steady profile is unstable.

2.1. An Energy Principle

Multiply the SMB (2.2) by $uf(u)$ and integrate, one gets the energy principle:

$$\frac{d}{dt} \int_0^L \sqrt{1+u^2} dx = 2 \int_0^L (\partial_x[uf(u)])^2 dx - \int_0^L f(u)(\partial_x^2[uf(u)])^2 dx. \quad (3)$$

On the right hand side, the first term is a growing force, while the second term is a decaying force. When $|u|$ is large, $f(u)$ is small and the second term will be dominated by the first term. In such a case, the solution will be ever growing. The integral $\int_0^L \sqrt{1+u^2} dx$ is equivalent to the L^1 norm:

$$\int_0^L |u| dx < \int_0^L \sqrt{1+u^2} dx < \int_0^L (|u| + 1) dx = \int_0^L |u| dx + L.$$

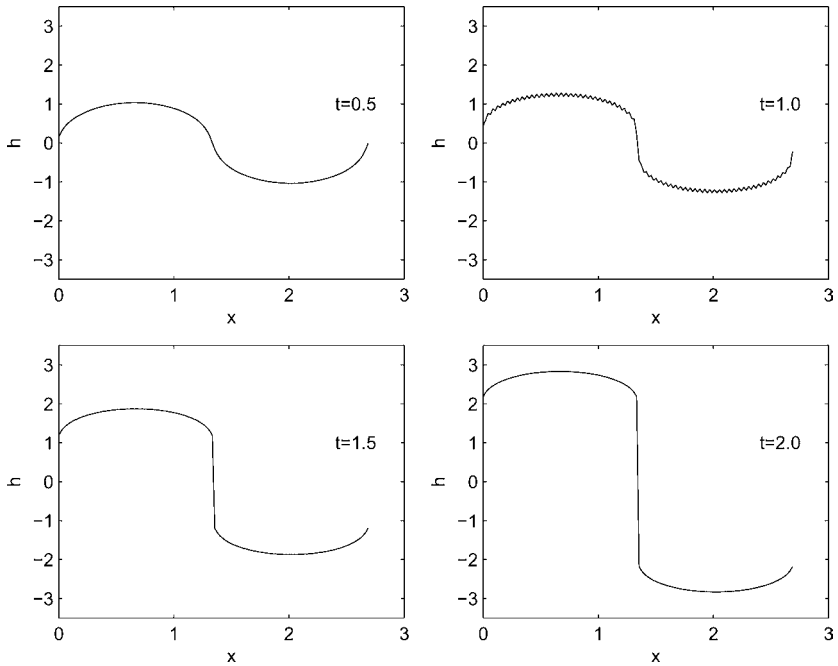


Fig. 8. Adding an explicit initial perturbation $0.1 \sin(\frac{2\pi}{\ell}x)$ to the initial steady state profile for $u_0 = 8.0$ in Fig. 7. The profile grows and develops a kink.

2.2. Linearization and Steady States

The zero state $u = 0$ is a trivial steady state. Linearization of the SMB (2.2) at $u = 0$ leads to

$$u_t = -2u_{xx} - u_{xxxx}.$$

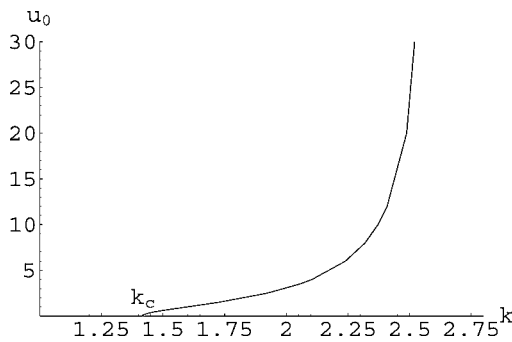


Fig. 9. The bifurcation diagram of the fixed points where $u_0 = \frac{w_0}{\sqrt{1-w_0^2}}$, $k = \frac{2\pi}{\ell}$, and $k_c = \frac{2\pi}{\ell_c} = \sqrt{2}$.

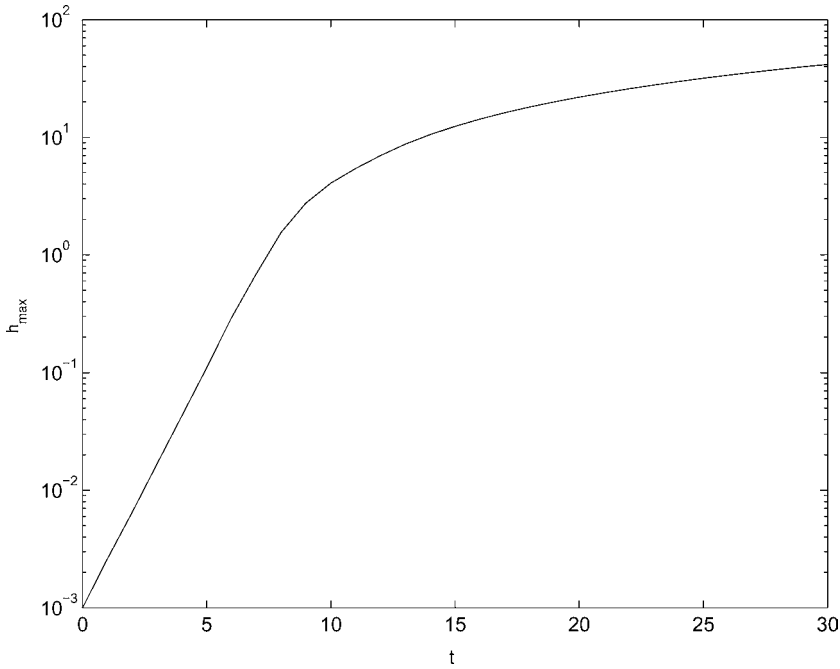


Fig. 10. The amplitude growth of the most unstable mode. The domain length $L = 20\pi$, the initial condition $h(0, x) = 0.001 \sin x$, $h_{\max} = \max_{x \in [0, L]} h(t, x)$.

Using the basic mode $u \sim e^{Wt+ikx}$, one obtains the dispersion relation

$$W = k^2(2 - k^2).$$

See Fig. 1 for its graph. The unstable bands are $k \in (-\sqrt{2}, 0) \cup (0, \sqrt{2})$. The most unstable modes are $k = \pm 1$. The width of the unstable bands is $\Delta k = \sqrt{2}$. Then the correlation length is $\ell_c = \frac{2\pi}{\Delta k} = \sqrt{2}\pi$. The aspect ratio is $\sigma = \frac{L}{\ell_c} = \frac{L}{\sqrt{2}\pi}$. In general, the steady states are governed by the equation

$$\partial_x^2 [f(u)(2u + \partial_x^2 [uf(u)])] = 0.$$

Under the periodic boundary condition, this implies that

$$2u + \partial_x^2 [uf(u)] = c\sqrt{1 + u^2}$$

where c is a constant. By the fact that u has zero mean,

$$c \int_0^L \sqrt{1 + u^2} dx = 0.$$

Thus $c = 0$, and the steady states are governed by

$$2u + \partial_x^2[uf(u)] = 0. \tag{4}$$

Introduce the new variable

$$w = uf(u) = \frac{u}{\sqrt{1+u^2}}, \quad w \in (-1, 1);$$

then

$$u = \frac{w}{\sqrt{1-w^2}}, \quad f(u) = \sqrt{1-w^2}.$$

Eq. (2.4) is transformed into

$$w'' + 2\frac{w}{\sqrt{1-w^2}} = 0. \tag{5}$$

Then

$$w^2 + V(w) = c \tag{6}$$

where c is a constant of integration, and $V(w) = -4\sqrt{1-w^2}$. For any periodic solution of (2.6), $c < 0$. An intuitive representation of the periodic solutions can be given by a ball sliding along the well $V(w)$ in Fig. 2. In the original SMB paper (p. 2373 ⁽⁴⁾), their so-called $c > 0$ steady states are not solutions (not steady states). It was such so-called steady states that they claimed stable.

For the initial condition: $w(0) = w_0, w'(0) = 0; c = -4\sqrt{1-w_0^2}$; the spatial period is

$$\ell = \frac{1}{2} \int_{-w_0}^{w_0} \frac{dw}{\sqrt{\sqrt{1-w^2} - \sqrt{1-w_0^2}}} = \int_0^{w_0} \frac{dw}{\sqrt{\sqrt{1-w^2} - \sqrt{1-w_0^2}}}.$$

Numerical calculation shows that for $w_0 \in (0, 1)$, ℓ is a decreasing function of w_0 , (Fig. 3). When $w_0 \rightarrow 0$, Eq. (2.5) reduces to

$$w'' + 2w = 0.$$

The period of the solutions to this equation is always $\sqrt{2}\pi$. Thus

$$\lim_{w_0 \rightarrow 0} \ell = \sqrt{2}\pi = \ell_c \quad (\text{correlation length defined above}).$$

The conclusion is that the spatial period of the steady states belongs to the interval $\ell \in (\ell_1, \ell_c)$ where $\ell_1 \approx 2.4$ and $\ell_c = \sqrt{2}\pi$, and the wave length of the unstable modes of $u = 0$ belongs to the interval $\ell = \frac{2\pi}{k} \in (\ell_c, +\infty)$. The two intervals have the common boundary point ℓ_c . Figs. 4–6 are some of the steady state profiles.

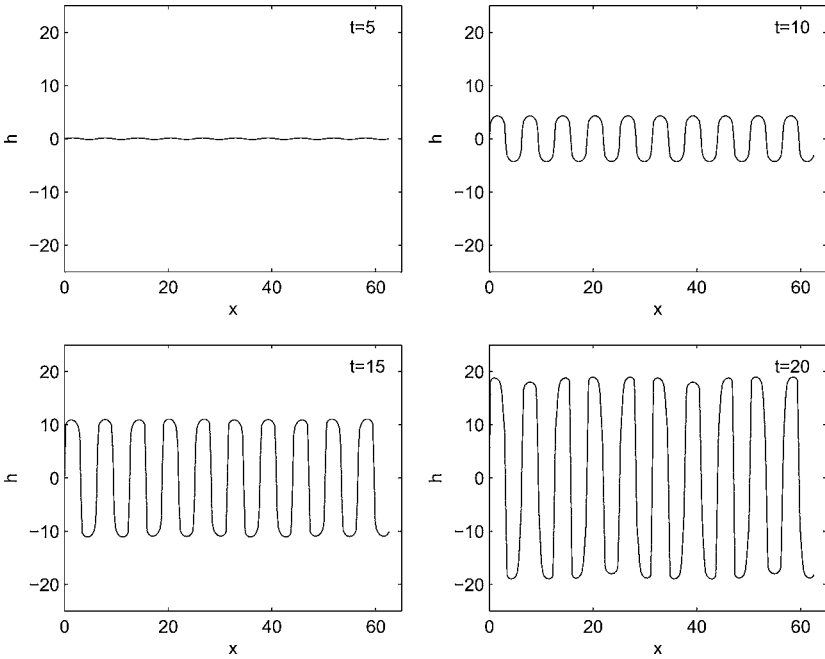


Fig. 11. Profile evolution of the most unstable mode in Fig. 10.

3. NUMERICS

Numerically we found that all the steady states are unstable. Figs. 7–8 show some of the profile evolutions. Kinks are developed during the evolutions. For each of the profile evolutions, we choose $L = \ell$ (the spatial period of the steady state). The initial perturbations also have the same spatial period $L = \ell$. The spatial period here only supports the stable modes of $u = 0$. Posing the SMB (2.2) on this spatial period $L = \ell$, $u = 0$ is a stable fixed point. The other nontrivial fixed point should be unstable. For different $\ell(k = \frac{2\pi}{\ell})$, the branch of the nontrivial fixed points in fact bifurcates from the $u = 0$ branch. See Fig. 9 for an illustration.

Next we choose $L = 2\pi$ and solve the original form (2.1) of SMB. We choose the initial condition

$$h(0, x) = 0.001 \cos x.$$

This corresponds to the most unstable mode of $h = 0$. The amplitude of the solution undergoes an exponential growth followed by a linear growth. See Fig. 10. If we rescale it by 10^{-3} , Fig. 10 will fit perfectly with the experimental data in [Figure 3 of ⁽³⁾]. The transition time from exponential growth to linear growth happens around $t = 10$ and is in agreement with the experiment too. We do not know if

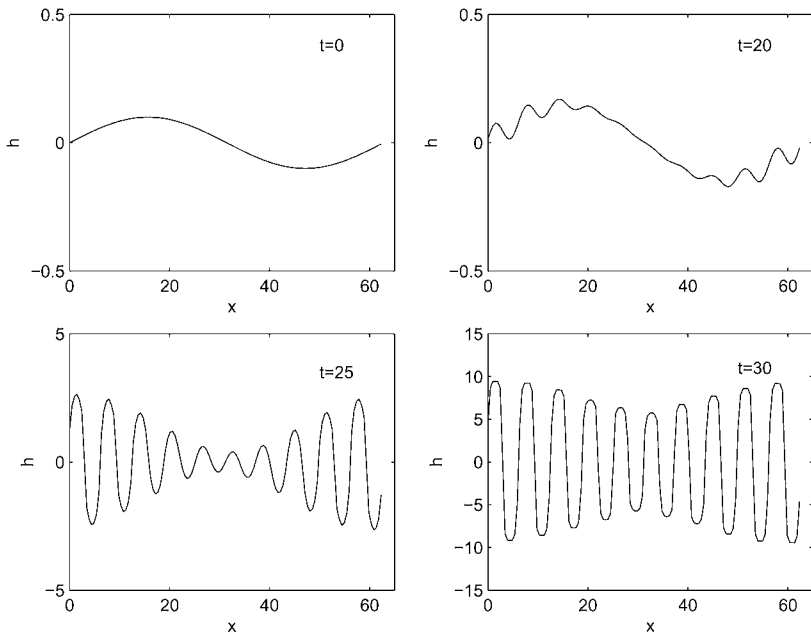


Fig. 12. Evolution of the solution starting from a small initial condition $h(0, x) = 0.1 \sin(0.1x)$ in a large aspect ratio domain.

the experimental data above have a scaling error. On the other hand, we never observed the decay portion of the numerical solution in [Figure 3 of ⁽³⁾]. Figure 11 shows the evolution of the profiles.

In the large aspect ratio case $L = 20\pi$ ($\sigma = \frac{L}{\ell_c} = 10\sqrt{2}$), starting from a small arbitrary initial condition, the most unstable mode ($k = 1$) of $h = 0$ quickly dominates, later on kinks are developed. See Fig. 12.

When the aspect ratio is decreased to less than $\sqrt{2}$, the $k = 1$ unstable mode of $h = 0$ can not be supported by the spatial domain. The next most unstable mode will replace $k = 1$ and behaves exactly the same as the $k = 1$ -most unstable mode above. For example, let $L = \frac{6}{5}\pi$ ($\sigma = \frac{3}{5}\sqrt{2}$), the most unstable mode of $h = 0$ is $k = \frac{6}{5}$. The $k = \frac{12}{5}$ mode will be stable. We start with the $k = \frac{12}{5}$ stable mode $h(0, x) = 0.5 \sin(12x/5)$. First the mode decays to near zero. Then computer error picks up the most unstable $k = \frac{6}{5}$ mode which grows again. See Fig. 13. Notice the development of kinks.

Of course, when the aspect ratio is less than 1, all modes of $h = 0$ are stable. Some of such spatial domains support other nontrivial steady states which are all unstable as shown above.

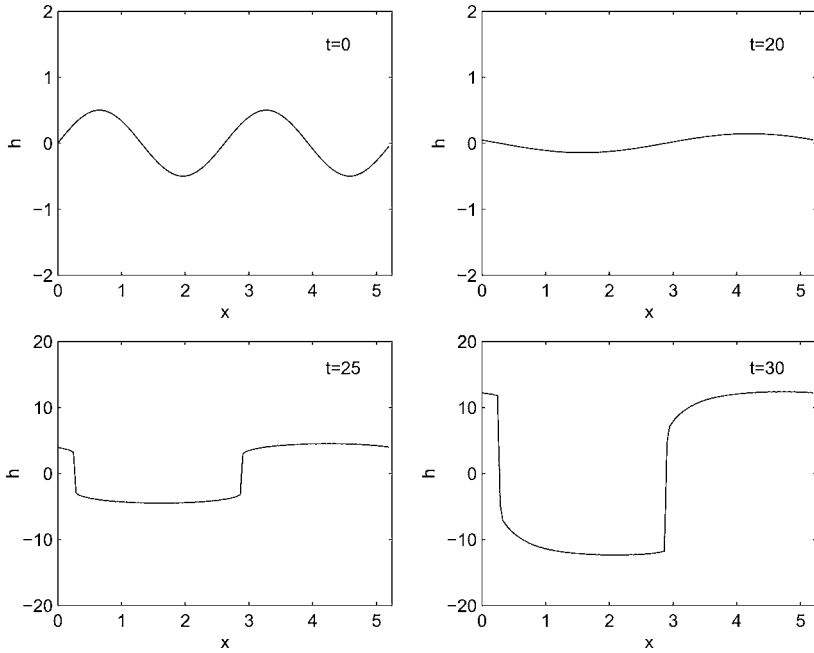


Fig. 13. The case of a domain which cannot support $k = 1$ most unstable mode. Specifically $L = \frac{6}{5}\pi$, starting from a $k = 12/5$ stable mode, when the mode decays near zero, the computer error picks up the most unstable mode $k = \frac{6}{5}$ which grows again.

4. CONCLUSION

Our main interest here is to solve the SMB equation. Our main finding is that typical solutions of the SMB equation are ever growing. The ever growing nature is in agreement with the experimental data [Figure 3 of ⁽³⁾]. We also find that all the nontrivial steady states are unstable. Therefore, saturations to steady states are impossible.

REFERENCES

1. S. Allen and J. Cahn, A microscope theory for antiphase boundary motion and its application to antiphase domain coarsening. *Acta Metall.* **27**:1085 (1979).
2. J. Cahn and J. Hilliard, Free energy of a nonuniform system. I., *J. Chem. Phys.* **28**:258 (1958).
3. J. Erlebacher *et al.*, Nonlinear amplitude evolution during spontaneous patterning of ionbombarded Si(001). *J. Vac. Sci. Technol.* **A18(1)**:115 (2000).
4. D. Srolovitz, A. Mazor and B. Bukiet, Analytical and numerical modeling of columnar evolution in thin films. *J. Vac. Sci. Technol.* **A6(4)**:2371 (1988).